

Experimental study of the interaction between thermal plumes and human breathing in an undisturbed indoor environment

Zhu Cheng^{a,*}, Guangyu Cao^b, Amar Aganovic^b, Baizhan Li^{c,d}

^a College of Architecture and Environment, Sichuan University, Chengdu, 610065, China

^b Norwegian University of Science and Technology (NTNU), Department of Energy and Process, Kolbjørn Hejes Vei 1B, NO-7491 Trondheim, Norway

^c Joint International Research Laboratory of Green Buildings and Built Environments, Ministry of Education, Chongqing University, Chongqing, 400045, China

^d National Center for International Research of Low-carbon and Green Buildings, Ministry of Science and Technology, Chongqing University, Chongqing, 400045, China

*Corresponding email: scchengzhu@126.com

Abstract: This study characterized the interaction between human thermal plume and breathing air flow while people are sitting in a quiescent indoor environment. A sitting breathing thermal manikin was developed to mimic a real human, and data from real human subjects was collected to verify the breathing thermal manikin. In this study the velocity and temperature were measured in front of and above the breathing thermal manikin with and without breathing. In addition, the breathing modes through mouth and nose were studied to investigate the influence of breathing mode on the development of thermal plume, respectively. The ambient temperature was set at $23\pm 0.5^{\circ}\text{C}$, and the surface temperature of manikin varied between $33\text{--}34^{\circ}\text{C}$. At a height above the head, the velocity reaches a maximum value and then starts to decrease with increase in height. Without breathing, a maximum value of 0.193m/s was reached at around 35cm height above the head which was 1% and 10% higher than the mouth-breathing case and nose breathing case, respectively. However, the breathing would weaken the thermal gradient and lower the maximum velocity and had little influence on the height of maximum velocity. Above the manikin's head, the velocity distribution in the non-breathing case showed little difference compared to the breathing cases. But the velocity above the head in the non-breathing case reported the highest maximum value and had the shortest height at which the maximum velocity was reached. Breathing through the nose had much more impact on airflow around manikin than breathing through the mouth, even change the flow direction.

Keywords: thermal plume; breathing thermal manikin; real human; sitting posture.

1. Introduction

When people perform normal activity, the average skin temperature is about 33--

34°C^{[1][2]}, and the body core temperature is at around 37°C^[3]. The indoor air design temperature range is 20-26°C^{[4][5]} which is approximately 7-14°C colder than the human average skin temperature. Because of the temperature difference between human skin and indoor air, the human body heat loss will generate thermal plume and convective boundary layer (CBL) near human body which have an impact on airflow and pollutant concentrations around people^{[6][7]}. Bjørn and Nielsen (2002) and Johnson et al. (1996) found that buoyant upward flow which around people has an impact on pollutant distribution in the breathing zone. Thermal plume created by the heat loss of the human body becomes a significant factor which has an impact on airflow and temperature in the indoor environment with little or no air mixing^{[8][9]}.

There are a lot of research on velocity generated by people's thermal plume. For a sitting person, the boundary layer is generated from the feet, but the lower part thermal plume generated from feet, knees, and thighs influences with the thermal plume generated from the upper part like abdomen which has many differences with standing posture. As a result, the convective flow in the region over the human face differs slightly for the standing posture compared to sitting posture^[10]. Due to the interaction between the thermal plume generated from the feet and body, the thermal plume 0.7m above a sitting person is asymmetrical^[11]. The increase of ambient temperature from 20 to 26°C widens the CBL flow in front of a sitting manikin and reduces the mean peak velocity from 0.24 to 0.16 m/s in the CBL^[12]. At room temperature average of 23°C, the mean vertical velocity in the breathing zone at a horizontal distance of 6 cm from the face, is 0.14m/s^[13]. A study has shown that loose clothing increases the volume flux by 24%, and so changes the shape of the plume. Also, the wig on the manikins head appears to be an important factor influencing the velocity field as a bald head has shown to decrease the volume flux by 15%^[14]. The velocity of the ascending airflow reaches its maximum value above the head at 0.23m/s at an indoor air temperature of 22°C^[9]. Without wig and clothing, and at an indoor temperature of 18°C, the maximum velocity above the manikin's head was slightly more than 0.3 m/s. While at 24°C, this velocity value decreases to 0.27 m/s, and at 30°C, the air velocity is measured at only 0.2 m/s^[15]. This study used hot-sphere anemometers placed along different vertical heights above

the subject's head and the maximum speed measured was approximate 0.23 m/s at around 23°C^[16]. A study has shown that at an ambient air temperature of 21.3°C, the maximum velocity of 0.24 m/s occurs at the height of 0.43m above the head, and by utilizing CFD methods, it has reported a maximum velocity of 0.20 m/s at the height of 0.39m above the head^[17].

Some researchers noticed that the body posture had significant effect on CBL. Several researchers^{[18][19]} have used Schlieren photography technique to visualize the growth of the CBL for different body postures. These studies showed that different body postures affect the development of the CBL around the body. Compared to the standing posture, the supine posture generates a weaker convection flow and different heat loss rates in the head region. The heat loss in the head region of a lying person reported 30% greater heat loss compared to the head region of a standing person. The influence of legs is minimal in supine position compared to a sitting and standing position, due to their relative horizontal position from the nostrils^[20]. The flow generated from a lying position is slower and thinner compared to the flow of standing and sitting position, and the strongest flow is formed around a standing position^[18]. As most of the working and relax time in daytime is spent in sitting posture, in this position the surrounding airflow disturbance due to movement of human body and disturbance in the surrounding environment is relatively negligible. Therefore, research on sitting posture is of practical significance.

Breathing through nose or mouth has different effect on the velocity and temperature around people. At low activity levels, almost all people exhale through the nose^[21]. In this case, two air jets with an intervening angle are formed towards the chest and diffuse similarly to two independent air jets in a room environment^{[22][23]}. In the quiescent environment, the temperature difference between the exhaled air, thermal plume, and the indoor air results in an upward movement of exhalation air from both the mouth and the nose. Hyldgaard's (1994)^[22] studies showed that the air exhaled through the nose almost always becomes part of the convective flow around the body, and only when people sit at a table with the head bent forward, the exhaled air can be pulled back to the chest. In another paper, Hyldgaard (1998)^[24] presented the air

velocity distribution in the thermal plume above the head of breathing and non-breathing, both sitting and standing, dressed thermal manikin. The measurements showed that breathing had hardly any effect on the velocity above the head when people exhaled air from the nose in a quiescent environment. Rim and Novoselac (2009)^[25] showed that the breathing of a sedentary thermal manikin (inhalation and exhalation both through the nose) has an influence on the airflow in the breathing zone but they confirmed that breathing only has a minimal effect on the thermal plume 0.25 m above the head in a room equipped with displacement ventilation.

The previous studies regarding human thermal plume have not clarified the influence of different breathing air flow mechanisms, especially in the breathing zone and above the head region in the case of a sitting posture. The investigation of the interaction between the thermal plume and breathing can provide data support for optimizing the breathing air quality. Moreover, only a few studies have used real human data to verify their manikin experimental measurements. This research focuses on the characteristic of thermal plume when people with wig and clothes sit in a quiescent indoor environment and aims to investigate the resulting temperature and velocity due to the interaction between the thermal plume and breathing air flow. This research can fill the gap of the thermal plume when sitting, and provide support to control the air quality in the breathing zone. The main objective of the present work is to characterize the human thermal plume, especially in breathing zone in a quiescent room environment.

2. Experimental setup

Experimental measurements were conducted in the Energy and Indoor Environment Laboratory at the Department of Energy and Process Engineering at NTNU, Trondheim, Norway. In this study, velocity, temperature and turbulence intensity in the breathing zone with a breathing thermal manikin are measured in an climate chamber. The following sections provide information about the experimental setup, breathing thermal manikin and test instruments.

2.1. Climate chamber

The experimental facility resembled an environmental chamber with dimensions 3.95m×2.35m×2.65m (L×W×H) as shown in Fig. 1. This chamber is equipped with the thermal manikin, chair, ventilation system, extracts, measurement apparatus. The extracts are placed about 0.3m from the ceiling and are about 1.0m from the side walls. The chair is set right down the center of the laminar air flow panel. During the experiments, the ventilation system was turned off with the aim to provide quiescent indoor conditions. However, the ventilation would be turned on after a set of test to keep the indoor temperature consistent. Ambient temperature was kept at $23\pm 0.5^{\circ}\text{C}$.

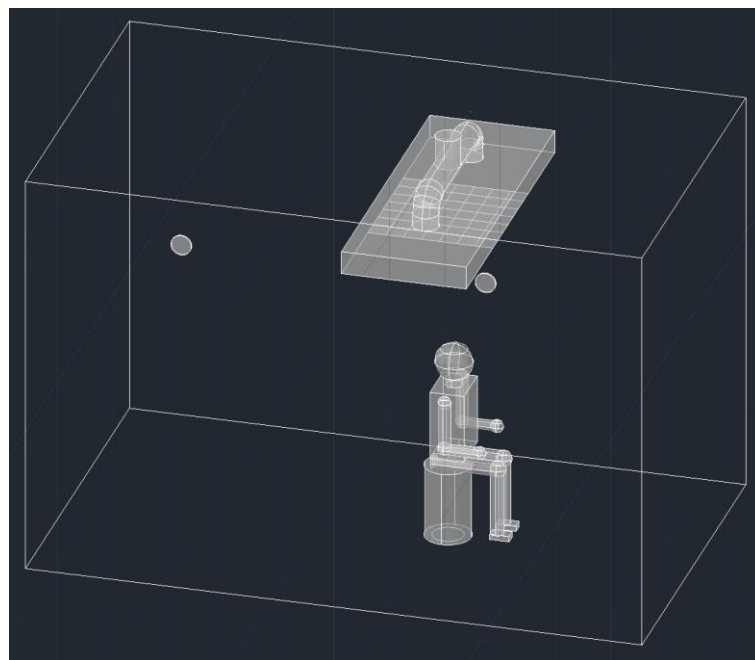


Fig. 1. The experiments in chamber.

2.2. Breathing thermal manikin and real human subject

To simulate the situation of the human, a breathing thermal manikins with complex female body shape was used to resemble the human body. The mode of the sitting female manikin is: Lo Lzm 09 Ada head (white), produced by Morten Finckenhagen Butikkinnredninger AS. It can simulate the skin temperature and sensible heat release of the human body with heating wires directly under their surface. The female manikin dressed in shirt and jeans was positioned in sitting posture with an insulation value of approximately 0.8clo. and was seated on a cylinder which had a height of 0.48m to minimize the impact of the chair. Real human (see in Section 3.3 Real human) kept the

same posture with the manikin.



Fig. 2. The breathing thermal manikin and a real human.

The female manikin had a height of 1.42m in the sitting posture. The manikin has a similar geometry to a real human and can move arms and legs, also can control the temperature of the leg, head, arm, and torso separately. The manikin's breathing system can provide realistic airflow associated with inhalation and exhalation. During the experiments, the manikin's body was kept at a surface temperature of around 33-34°C, and heat loss of this manikin is 113W. These scenarios were chosen to determine the effect of each parameter studied precisely.

Table 1 Summary of the experiments with different parameters (Fig. 2).

Parameter	Conditions	Details/comments
Ambient	23±0.5°C	-
Manikin heat output	113W	33-34°C
Body posture	sitting	Upright
Clothing	Thick loose clothing	Tight jeans, thick loose long-sleeve shirt
	Wig	Short hair wig, slightly below the ear level
Chair	Cylinder	0.48m height
Breathing	Mouth	See Table 3
	Nose	

Table 2 Summary of the real human subjects characteristics.

Parameter	Mean	SD
Height (cm)	162.25	6.39
Weight (kg)	52.63	3.63
Sitting height (cm)	125.67	5.13

In this research, the artificial breathing device is set up to simulate the real breathing human as the breathing zone area is of primary interest. The artificial lungs of the breathing thermal manikin simulated the breathing cycle of an average healthy person. Two fans are placed (AD0912DX-A76GL, ADDA Corp., Ltd) inside the head to simulate inhalation and exhalation respectively. The controllers (NI 9481 and NI 9203, National Instruments Corp.) are connected in parallel to the circuit and control the fan speed by controlling the current. The software of the system is Lab VIEW (version 12.0f3, National Instruments Corp.). The use of breathing system in the manikin was not used during the non-breathing measurements.

Table 3 Parameters of breathing thermal manikin.

Frequency of breathing (time/min)	air flow (L/min)	Mouth area (cm ²)	Nose area (cm ²)
17.5	8.61	1.20	0.70

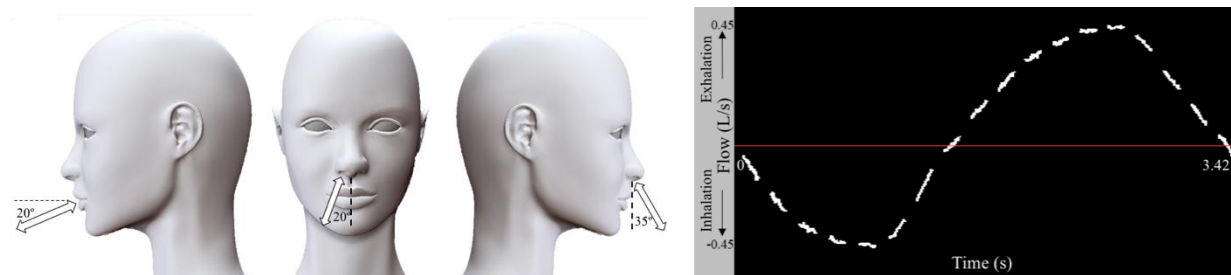


Fig. 3. Angles of breathing modes (left) and the breathing function of the manikin (right).

2.3. Measurement instrumentations

The instrument characteristics for measuring velocity, temperature and turbulence intensity are shown in Table 4. The air velocity measurement system used is “AirDistSys5000”, delivered by Sensor-electronic. The system consists of a pressure sensor that corrects anemometer readings according to the barometric pressure, five omnidirectional anemometer probes, a wireless transmitter that transmits the readings to a USB interface that is connected to a computer and a power supply. Sensor-electronic provides software to read and log recorded data.

Table 4 Parameters of the measuring instruments.

Model	Measuring variable	Range	Accuracy	Resolution
SensoAnemo5100LSF	Velocity	0.05-5m/s	$\pm 0.02\text{m/s}$ or $\pm 1.5\%$ of readings	0.001m/s
SensoAnemo5100LSF	Temperature	-10°C-50°C	$\pm 0.2^\circ\text{C}$	0.1°C
SensoBar 5301	Pressure	500-1500hPa	$\pm 3\text{hPa}$	1hPa

2.4. Measurement scenarios

Both velocity and temperature measurements took place at 11 different vertical locations and two lateral locations around sitting manikin (Fig. 4). Occupational Safety and Health Administration (OSHA)^[26] defines the breathing zone as an area within a 25cm radius of the people's nose and mouth, and U.S. Department of Energy^[27] defining the breathing zone as a hemisphere forward of the shoulders, centered on the mouth and nose, with a radius of 15 to 23cm. Therefore, in this study, breathing zone is defined as the within 10cm.

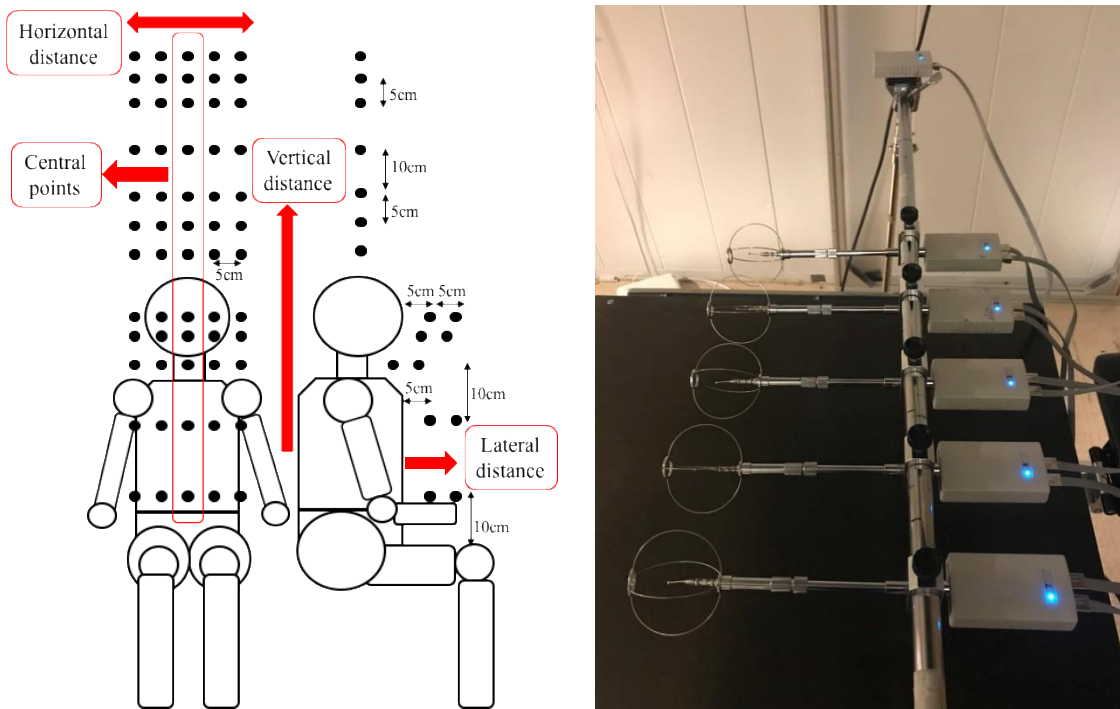


Fig. 4. The placement of sensors.

The mean velocity was obtained as an average of 90 single measurements of instantaneous velocity during 3 min. When the magnitude of the mean velocity was below 0.05 m/s, we indicated that quiescent indoor environment had been achieved, as suggested by Murakami et al. (2000)^[9].

There were five cases in this research (Table 5). The manikin was used in first three cases to investigate the characteristic of the thermal plume and the interaction between breathing airflow and thermal plume. The first case was to investigate the velocity and temperature generated by heat loss of manikin without breathing, case 2 and case 3 were to investigate the influence of breathing airflow on velocity and temperature. The real human was used in the last two cases to verify the manikin data.

Table 5 Detail of different cases.

Scenario	Subject	Detail
Case 1	Manikin	Without breathing
Case 2		Mouth breathing
Case 3		Nose breathing
Case 4	Real human	Mouth breathing
Case 5		Nose breathing

3. Results and discussion

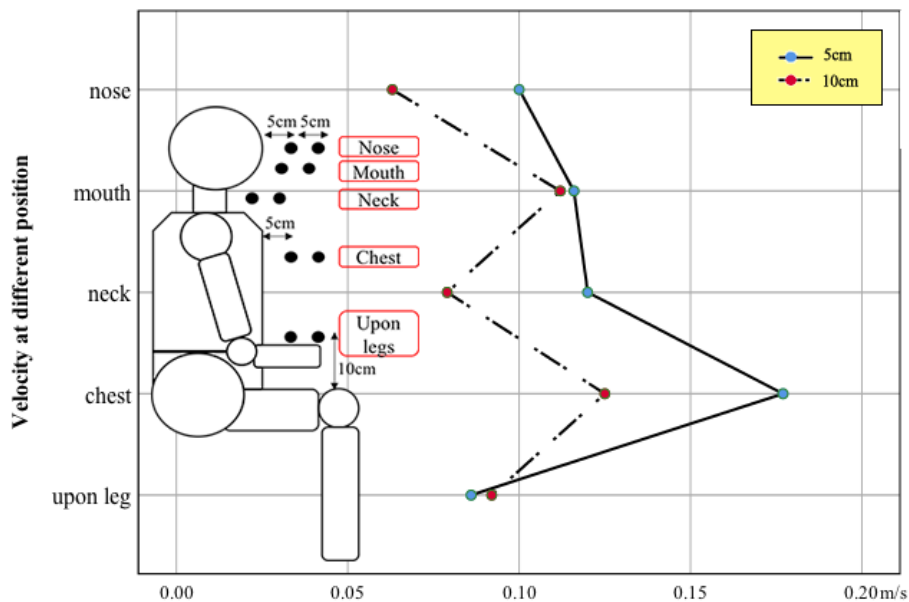
According to the subject and breathing mode (Table 5.), the experimental setup consisted of two different cases, each performed with different breathing modes, resulting in a total of 5 scenarios. After the measurements were completed on the thermal manikin, data readings from a real human are used to verify the data obtained from the thermal manikin readings.

3.1. Velocity measurements

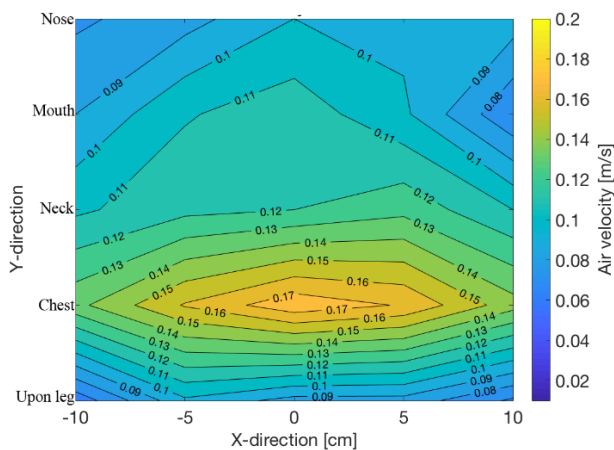
3.1.1. Sitting manikin without breathing mode

The measured velocity distribution is shown at five different heights measured a 5 and 10 cm lateral distance from the manikin's surface (Fig 5.) At a 5cm distance, the airflow velocity increases along to the chest with height, and then the velocity drops at nose region. At a 10cm distance, the velocity is lower than the velocity at the 5cm distance, and there is a little difference in the in the region close to the neck and mouth. This observation might be explained because the flow generated in the plume close to the leg and chest region is significantly stronger than at 5cm distance for the sitting position. The velocity reduction at the chin level at neck height may be attributed to a similar study showing the contours of the head behaving like a physical obstacle, as

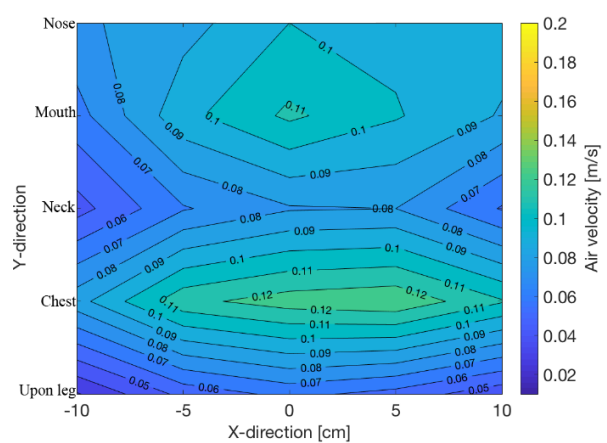
described by Lewis et al. (1969)^[28]. At a temperature of 23°C, the maximum velocity of the sitting manikin is observed at the height of chest and is equal to 0.177m/s. This result different compared to the one from previous research^[12] where the sitting manikin leaned 15°. The velocity increases with increase in the height of measurement points above the head, where the flow becomes detached and fully formed into the human thermal plume. The velocities reported at different height are different for the two manikins. This observation might be explained due to the difference in body shape as the sitting manikin is shaped like a female. With thick clothing, the maximum velocity in the breathing zone is 0.124m/s as similarly reported in a previous study^[12]. The measurements also show similar results in front of the mouth 0.116m/s and 0.112m/s at 5cm and 10cm distance respectively.



(a) Central point velocity difference at different lateral distances from the manikin.



(b) 5cm in front of the manikin.

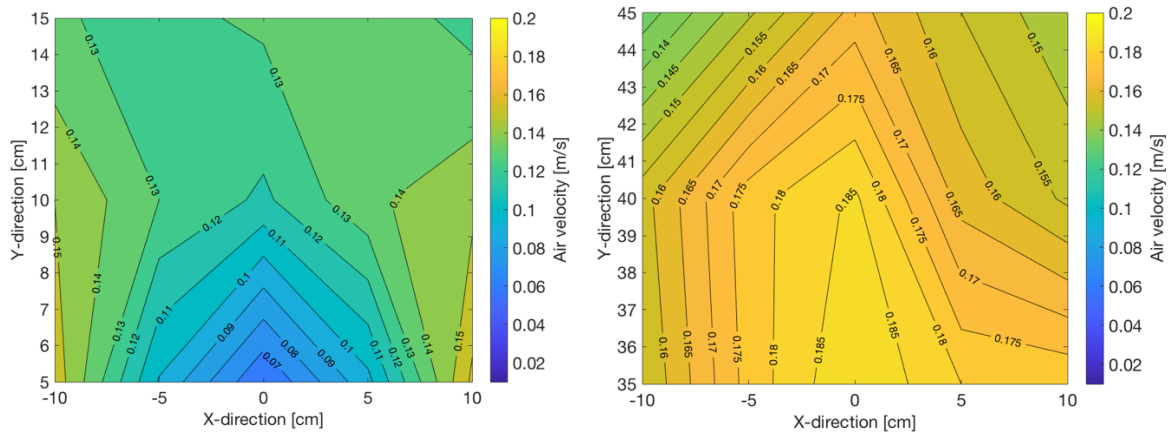


(c) 10cm in front of the manikin.

Fig. 5. Velocity profiles at different positions (non-breathing mode).

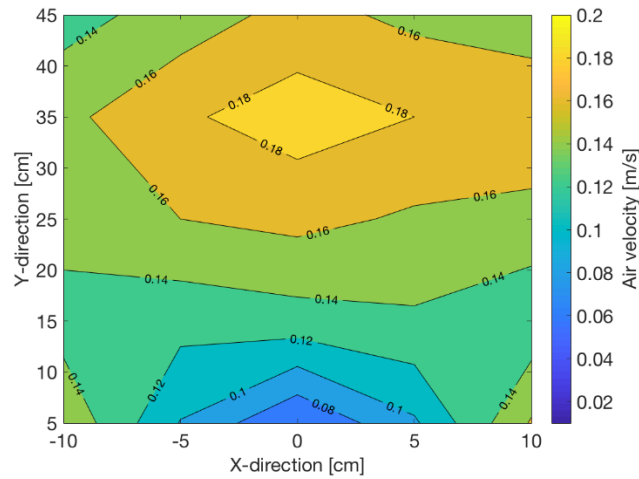
The central point velocity above the manikins head increases with the increased height (Fig 6), where the velocity reaches its highest value of 0.193 m/s at the height of 35 cm. With further increase in height, the velocities become lower as similarly reported in a previous study [17]. Due to the curved shape of the human's head, at a 5cm height above the head, the CBL still exists at the central point. However, this is not the case for other points at the same horizontal distance. The central point has the lowest velocity 0.06m/s.

At all the heights in front of the sitting manikin, the highest velocity is reported in the central point, but the data show some differences as the angle and height of forearm of manikin's left and right arm are not the same. This difference influences the velocities more at the region above the leg compared to the chest and neck region. Also, the velocities reported higher values at a lateral distance of 5cm compared to 10 cm. Due to the female body shape, at the height of chest, velocity is higher compared to other points. At the lateral distance of 5cm from the body, the velocity at the neck position is higher than at mouth position. This is not the case for at the measured points at a lateral distance of 10cm, because the sensor is located below the chin that may cause high turbulence which can affect the velocity.



(a) 5-15cm above the head.

(b) 35-45cm above the head.



(c) 5-45cm above the head.

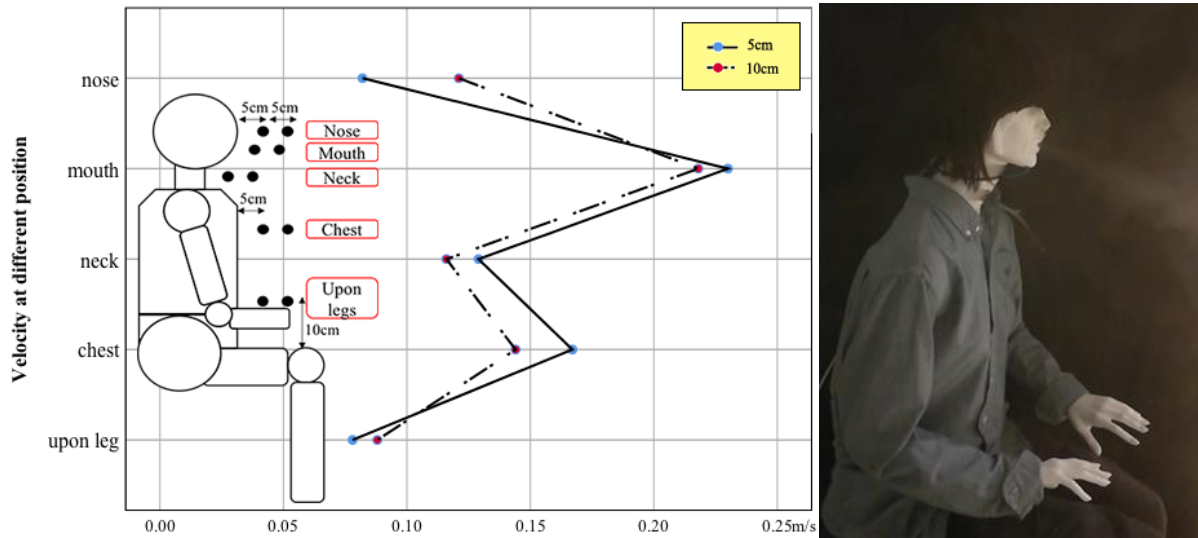
Fig. 6. Velocity profiles above the head (non-breathing mode).

3.1.2. Sitting manikin with breathing mode

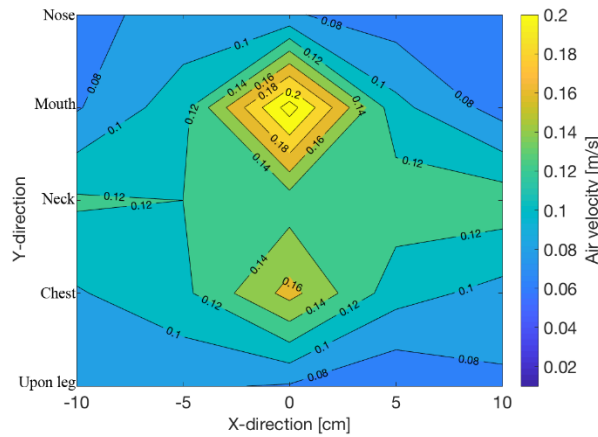
All the experimental situations are the same as in section 3.1.1, except the breathing mode which is active in these cases. The influence of nose and mouth breathing modes are studied separately.

1) Mouth breathing mode

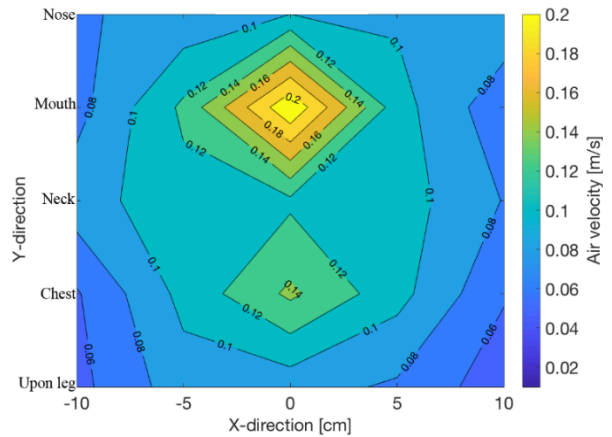
Experimental measurements were conducted at two different lateral distances 5 and 10cm from the manikin at different heights (Fig. 7). As the height increases, the air flow velocity accelerates up to the chest and decreases in the proximity of neck region. Due to breathing effect, at mouth height level, the velocity increases up to the maximum value and then drops dramatically to the value at nose height level. At the 10cm lateral distance from the manikin, the velocity is lower than that at the 5cm lateral distance except at the nose height level and above legs. The breathing influence also ceases the increasing trend of velocity at nose height. Also, the velocity at the nose height level is lower at the 5cm lateral distance. At 23 °C ambient temperature, the maximum velocity generated by the thermal plume of the sitting manikin is observed at the chest height level, which is equal to 0.167m/s. The velocity at mouth height is 0.230m/s due to the mouth breathing.



(a) Central point velocity difference at different lateral distances from the manikin.



(b) 5cm in front of the manikin.



(c) 10cm in front of the manikin.

Fig. 7. Velocity profiles at different positions (mouth breathing mode).

For the sitting manikin with mouth breathing effect, the central point velocity is lower than the case without breathing except at mouth height level. Furthermore, the air flow velocity at the height of mouth and chest is not uniform as the horizontal distance changes for both lateral distances 5 and 10cm from the manikin due to breathing effect. However, the air flow velocity at different heights is higher for the point at 5cm lateral distance in comparison with those at 10 cm lateral distance.

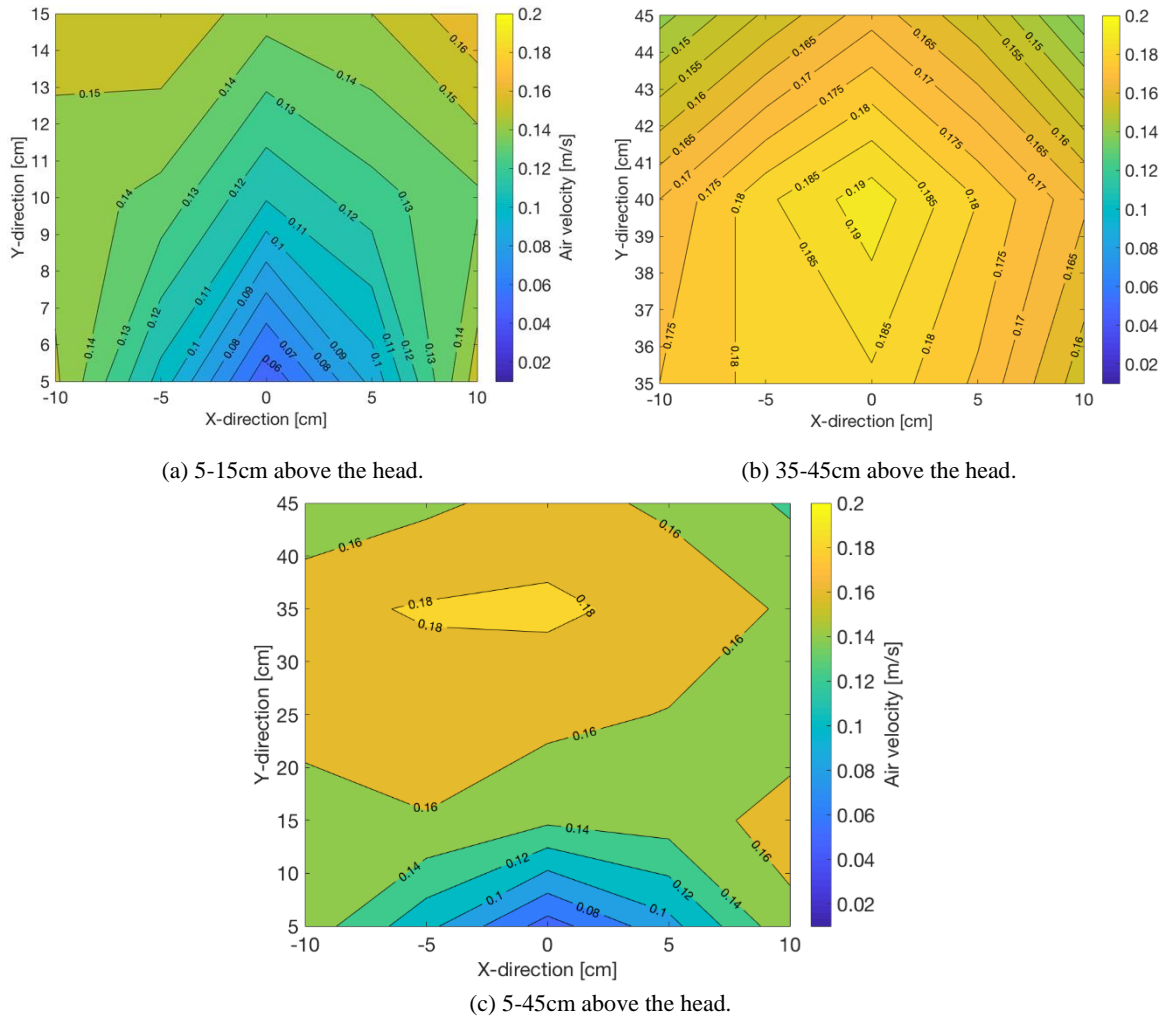


Fig. 8. Velocity profiles above the head (mouth breathing mode).

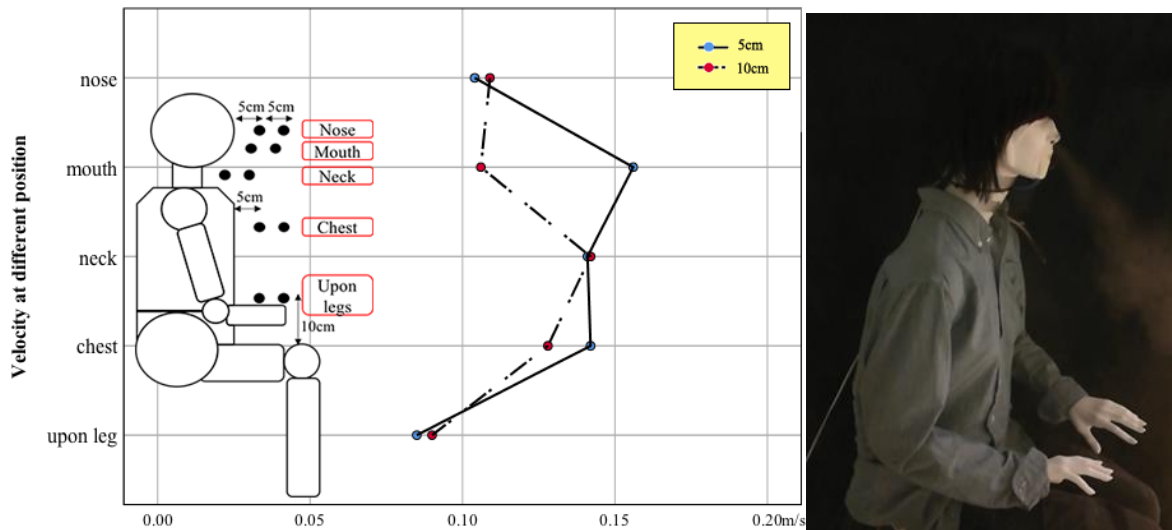
As Fig. 8 shows, the central point velocity above the manikin's head increases as the measuring height increases, which is the same as the case without breathing effect. The velocity reaches the highest value 0.191 m/s at the height of 40 cm and it drops when the height is over 40 cm. The distribution of velocity above the head in the vertical distance is very similar to that without breathing case. The maximum central point velocity is also the same with and without breathing effect. However, the vertical distance from the head at which the maximum velocity occurs is larger for the case without breathing effect.

2) Nose breathing mode

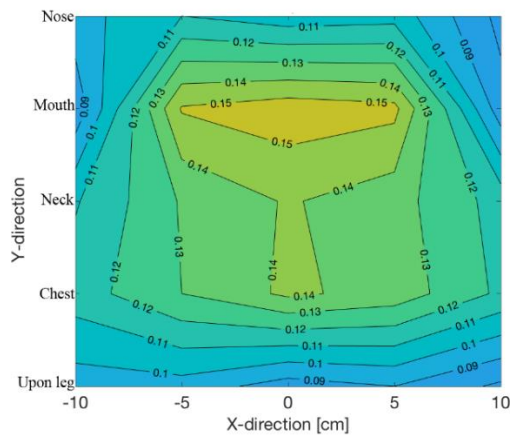
Experimental results were measured at two different lateral distances 5 and 10 cm from the manikin at different heights (Fig. 9). Similar to the mouth breathing case, the air velocity accelerates up to the chest height and then drops at the neck height level.

The same trend of air velocity profile as the mouth breathing is observed. The velocity at nose, neck, and legs level is higher at a 10cm lateral distance compared to 5cm lateral distance. At a 5cm lateral distance, the velocity increases at mouth height level up to maximum value because the mouth measuring point is located in the effective downwards breathing jet region. However, a decreasing trend is observed at mouth height level 10cm lateral distance from manikin because the measuring point is located outside of the effective breathing jet region.

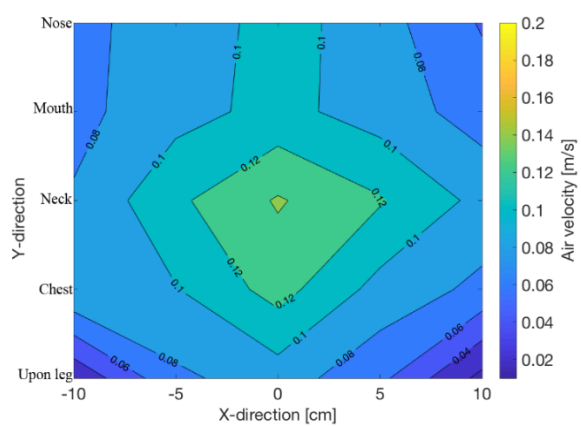
At 23°C ambient temperature, the central point velocity is 0.142m/s which is influenced mostly by the upward thermal plume at the height of chest, while the velocity at mouth height is mostly affected by the downward jet, which is equal to 0.156m/s.



(a) Central point velocity difference at different lateral distances from the manikin.



(b) 5cm in front of the manikin.

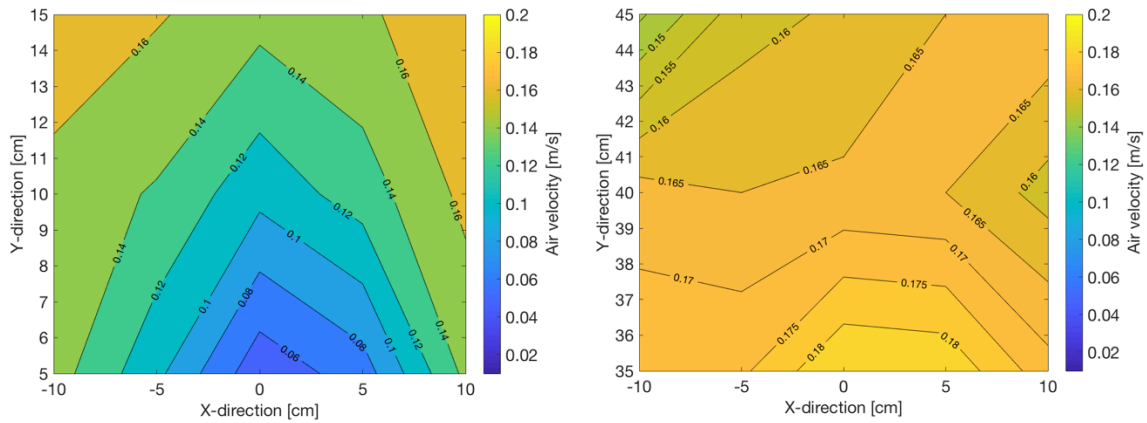


(c) 10cm in front of the manikin.

Fig. 9. Velocity profiles at different positions (nose breathing mode).

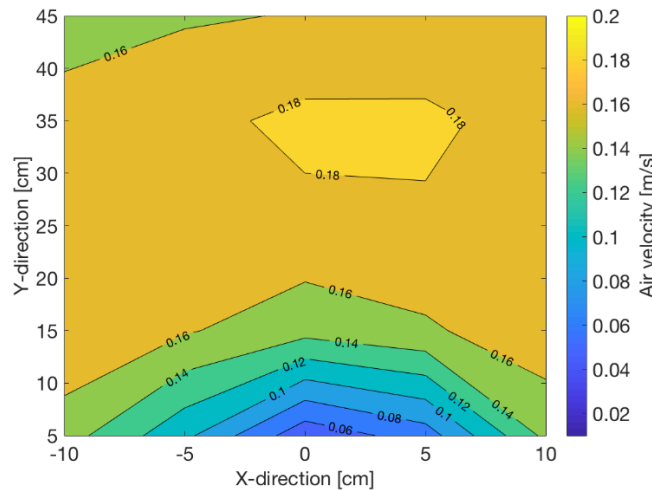
In Fig. 10, the central point velocity above the manikin's head shows the same

distribution as the same with non-breathing case and mouth breathing case. The central point velocity reaches the maximum value 0.174m/s at the height of 35cm, and the velocity drops when the vertical height increases above 35cm. The maximum central point velocity value is lower than that without breathing as well as with mouth breathing cases. The vertical distance from the head to the point where the maximum velocity occurs in nose breathing case is lower than that in the mouth breathing case and is very similar to the vertical distance in the case without breathing. Furthermore, breathing through the nose has more influence on the velocity value above the head than mouth breathing case.



(a) 5-15cm above the head.

(b) 35-45cm above the head.



(c) 5-45cm above the head.

Fig. 10. Velocity profiles above the head (nose breathing mode).

3.2. Temperature measurements

3.2.1. Sitting manikin without breathing mode

Temperature above the manikin's head drops as the height increases, and the

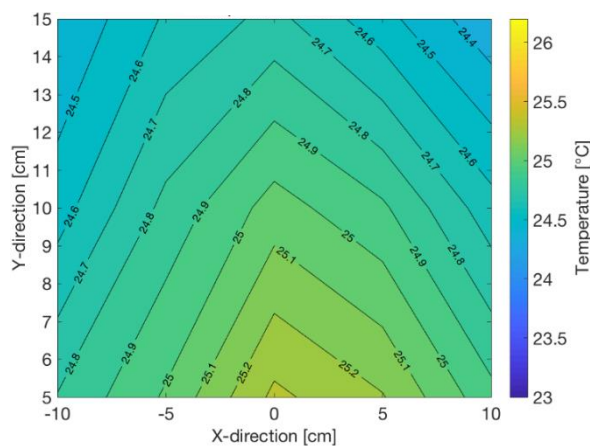
central point always has the highest temperature in the same horizontal direction. At the height 45cm, the temperature is similar to the indoor air temperature (Fig. 11).

At the different height in front of sitting manikin, the temperature drops as the lateral distance from the manikin increases (Fig. 12). The temperature above legs has the highest value because it is influenced by the legs, forearms, and abdomen. At the 10cm lateral direction from the manikin, the temperature is uniform at a same vertical distance, except for the temperature above legs, because of the thigh impacts on the temperature above the legs.

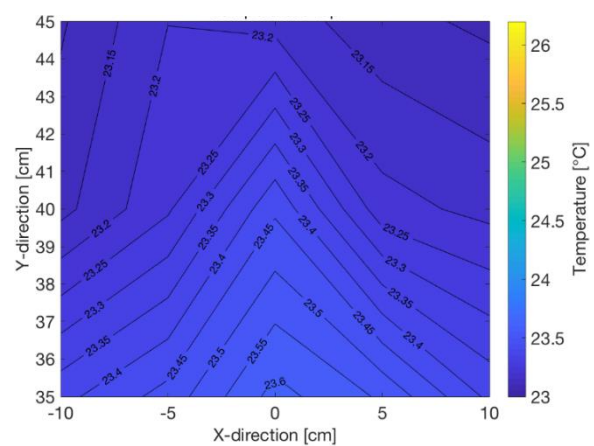
In this study, the thickness of the thermal boundary layer was defined as the distance between the surface temperature to the point the temperature drops to indoor air temperature. In other words, the thickness was assumed that the outer edge of the thermal boundary layer extends to a distance where the air temperature drops 90% from the temperature of the surface of the manikin to the temperature of the indoor air^[29]. The air temperature at the outer edge of the thermal boundary layer was determined as follows:

$$T_{TBL} = T_{surf} - 0.9 \times (T_{surf} - T_{amb})$$

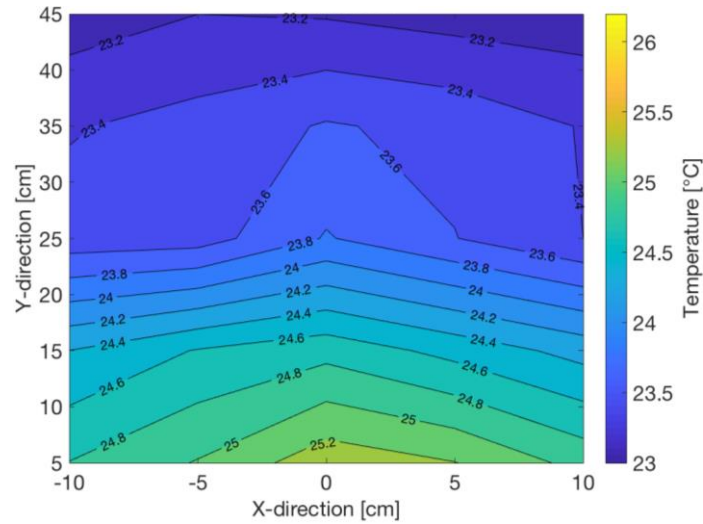
Where the T_{TBL} is the temperature at the outer edge of the thermal boundary layer, the T_{surf} is the temperature at the surface of the manikin, and the T_{amb} is the indoor air temperature.



(a) 5-15cm above the head.

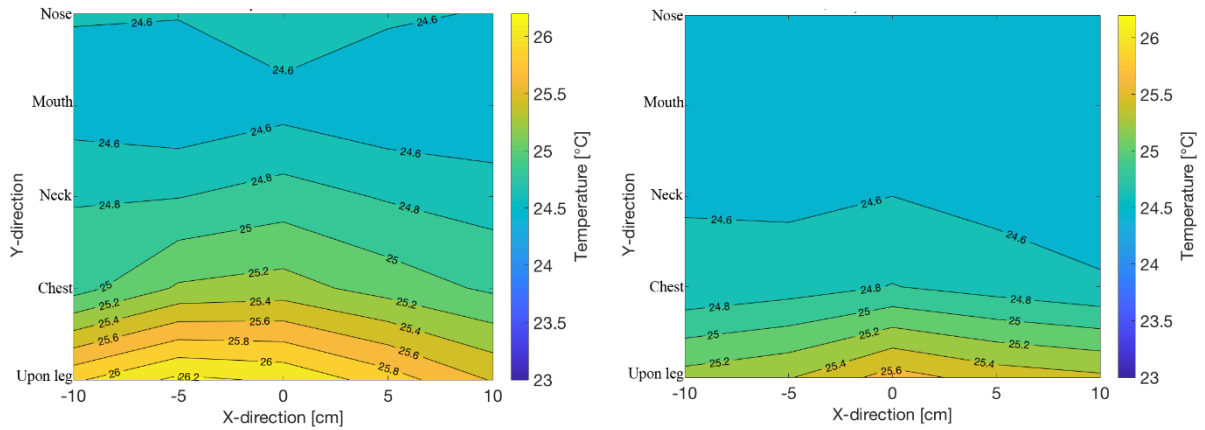


(b) 35-45cm above the head.



(c) 5-45cm above the head.

Fig. 11. Temperature profiles above the head (non-breathing mode).



(a) 5cm in front of the manikin.

(b) 10cm in front of the manikin.

Fig. 12. Temperature profiles at different positions (non-breathing mode).

At the 5cm vertical distance above the manikin's head, the temperature is higher than the T_{TBL} , but at 10cm vertical distance above the head, the temperature is lower than the T_{TBL} . It means that the thickness of thermal boundary layer above head is the between 5cm and 10cm.

At the 5cm lateral distance from the manikin, the temperature at mouth height and nose height is lower than the T_{TBL} which means the thickness of thermal boundary layer at these two heights is not reached to 5cm. At other height, the temperature is higher than the T_{TBL} , the thickness at these positions is larger than 5cm.

At the 10cm lateral distance from the manikin, the temperature at chest height level and above leg is more than the T_{TBL} implying the thickness of thermal boundary layer at these two heights is more than 10cm. At the neck height level, the temperature

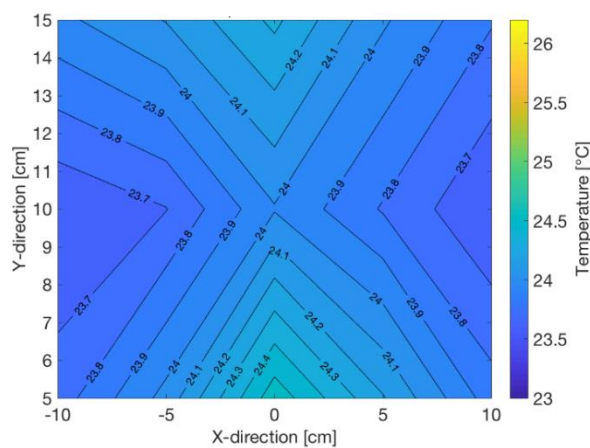
is lower than T_{TBL} , so the thermal boundary thickness is between 5cm to 10cm. The results are similar to the previous study conducted by Licina (2015)^[29].

3.2.2. Sitting manikin with breathing mode

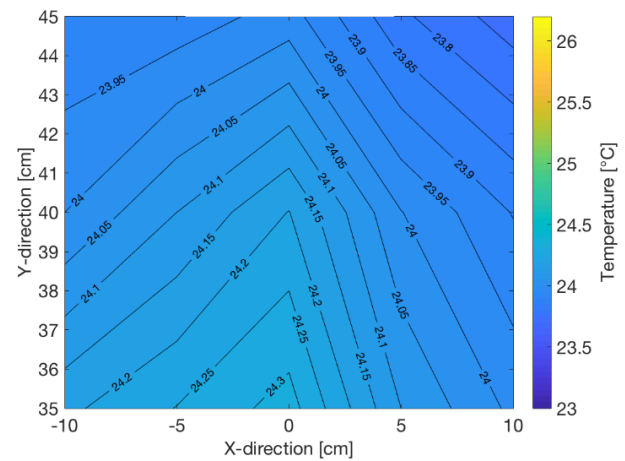
1) Mouth breathing mode

Above the head, the temperature first drops as the height increases to 25cm from the head, then the temperature increases to the 35cm from the head and drops again as the height increases (Fig. 13). But, at the 45cm height, the temperature is 0.9°C higher than the indoor air temperature which is different from the non-breathing case. The mouth breathing influences the temperature above the head so that the temperature distribution changes compared to the non-breathing case. The temperature gradient is also smaller than the non-breathing case.

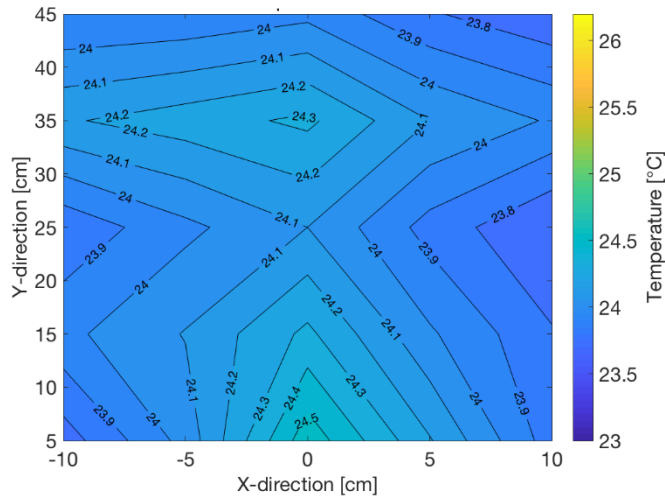
At the different height in front of the sitting manikin (Fig. 14), the temperature reduces as the lateral distance increases. The temperature above legs has the second-high value; the highest value is at the mouth height. At a 10cm lateral distance from the manikin, temperature above legs has the highest value, because this area is influenced by the interaction of the plume generated by thigh as well as the turbulence generated by mouth breathing. A high-temperature region can be observed in front of the mouth due to the impact of warm mouth breathing jet. The central line temperature in front of manikin in vertical distance reaches the highest value compared to the temperature of other points at the same horizontal position due to the stronger influence of breathing experienced by the central line, especially at the chest and neck height level.



(a) 5-15cm above the head.

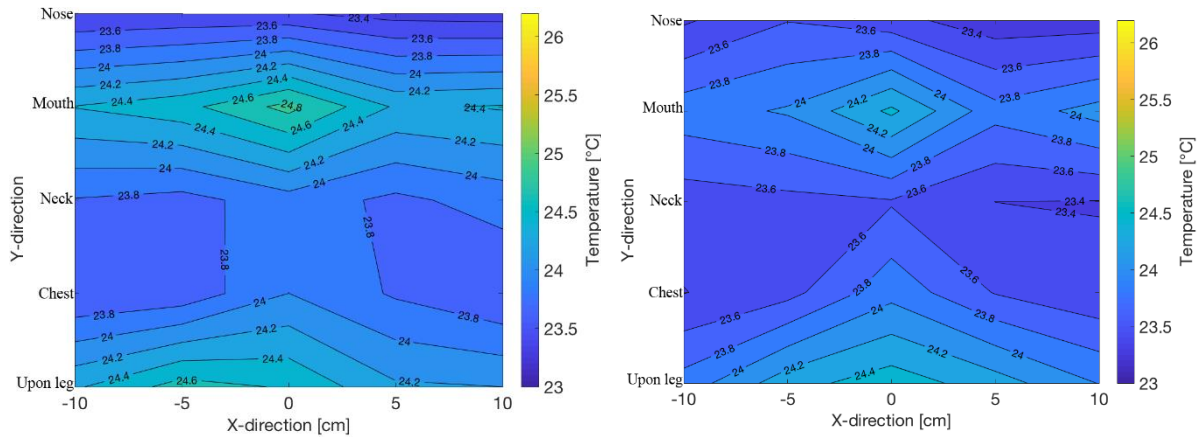


(b) 35-45cm above the head.



(c) 5-45cm above the head.

Fig. 13. Temperature profiles above the head (mouth breathing mode).



(a) 5cm in front of the manikin.

(b) 10cm in front of the manikin.

Fig. 14. Temperature profiles at different positions (mouth breathing mode).

2) Breathing through nose mode

As the height increases, the temperature in nose breathing case has the same changes and same distributions as the mouth breathing case (Fig. 15). But, the nose breathing airflow has more influence on the temperature than mouth breathing airflow. In nose breathing case, the maximum and minimum temperatures above the head are both lower compared to the mouth breathing case.

At the different height in front of the sitting manikin (Fig. 16), the temperature drops when the lateral distance from the manikin increases which is the same as the mouth breathing case. Due to the high temperature of breathing air flow, the temperature at mouth height level is higher than other positions. The temperature in front of the manikin is higher compared to mouth breathing case. At the 10cm lateral direction from the manikin, the temperature is uniform at a same horizontal distance

except for the position above the legs. Above the legs region, the interaction of breathing and thigh impacts the temperature value. Due to the higher speed as well as an oblique direction of breathing jet caused by nose in comparison with mouth breathing jet, nose breathing has a stronger impact on the temperature distribution in front of the manikin. At different lateral distances from manikin, measuring points on the edges of the horizontal direction experience lower temperature compared to mouth breathing case.

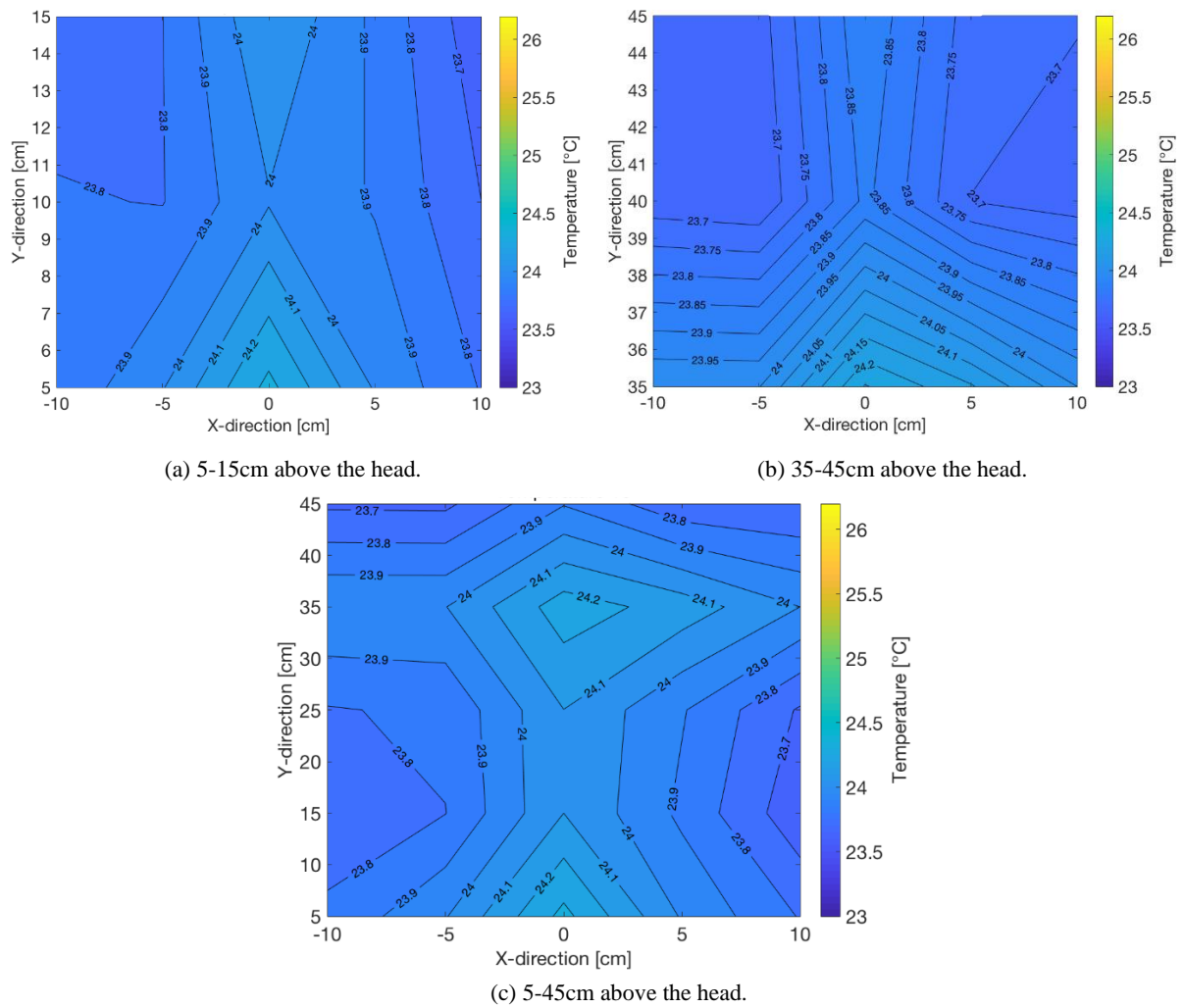
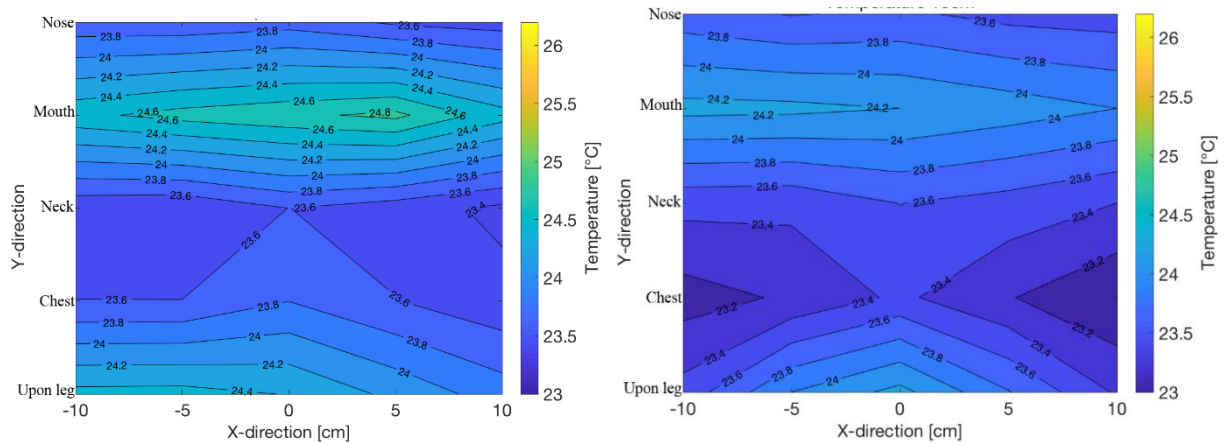


Fig. 15. Temperature profiles above the head (nose breathing mode).



(a) 5cm in front of the manikin.

(b) 10cm in front of the manikin.

Fig. 16. Temperature profiles at different positions (nose breathing mode).

3.3. Real human measurements

All the experimental situations with breathing manikin were replicated for the real human (Fig. 2), and six different vertical positions were selected to verify the data collected by manikin measurements. In these measurements, experiments were performed for nose and mouth breathing respectively. In these cases, it was decided to not use the measuring points in the breathing zone because it was hard for different people to control their breathing angle and frequency at the same level. Four different female subjects were measured with the same posture as sitting manikin. All the people wore tight trousers or jeans, and thick loose long-sleeve shirt, the characteristics of the people were shown in Table 2. All the measuring points were located in front of 5cm lateral distance from the body and at 5cm, 20cm, 35cm vertical distance above the head respectively. The central points values were used to compare with manikin's data.

The measured data were analyzed by the statistical method (SPSS, Version 25, IBM Corp.) with a significance level of $p=0.05$ and the velocity at each height can get a range of value.

In Fig. 17, as the height increases, the trend of velocity in the real human case is the same as the manikin case. The mean velocity of each point in the real human case is very similar to the velocity in manikin cases. In mouth breathing case, the velocity obtained from the manikin measurements is placed within the range of real human's data for all points. However, in nose breathing case, the velocity at 5cm above the head is not located within the limit since the velocity values for the points above the head

are relatively small compared to the real human velocity values that might be because of the different characteristics between the wig and real hair. At the height of leg, the range of the velocity is wide that might be resulted by the different heights of different people; longer legs and arms may generate more heat loss and larger velocity. Overall, the velocity of all the manikin measuring points is in the range except for one point, which implies that the heat loss of manikin is very similar to real human.

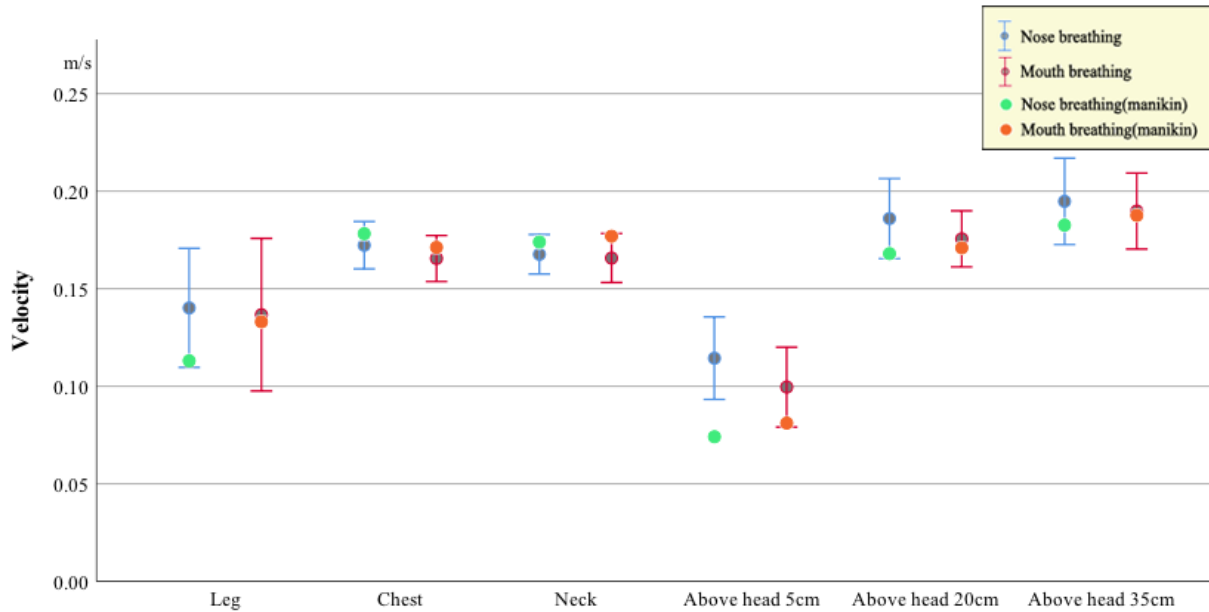


Fig. 17. Velocity values in different cases.

Experimental results show that the manikin is a suitable alternative for simulating the real human heat loss. However, the heat loss of the manikin caused by the wig (above the head) may have a little difference with the real situation.

3.4. Comparison of different manikin cases

The results of this study can provide a fundamental knowledge of airflow distribution in front of and above the human body. The finding reported in this paper confirms the previous results in the literature^[17]: the central point velocity above the head increases with height, and when reaches its maximum value, the central point velocity decreases sharply. Compared with previous studies, because of the lower temperature difference between the ambient air and surface of manikin^{[9][12][17]}, the peak velocities in front of the manikin and above the manikin are all lower.

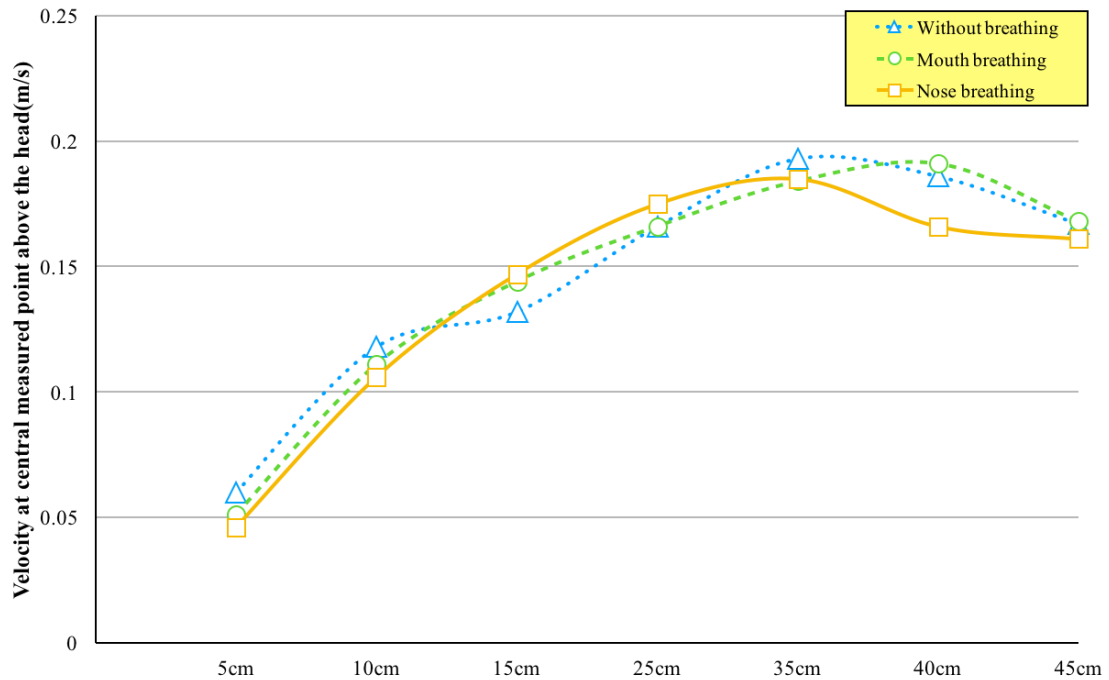


Fig. 18. Velocity at the central measured point above the head.

Taking account of the effect of breathing in experiments weakened the thermal gradient. In the mouth breathing case, the maximum velocity generated by thermal plume is 0.167m/s at chest height, which is 5% lower than the maximum velocity in non-breathing case. In nose breathing case, due to the downward airflow caused by nose exhalation, the direction of velocity at the chest height level is downwards, the velocity is -0.142m/s at chest height level which is 180% lower than the maximum velocity in non-breathing case.

Compared to the breathing case, the non-breathing case generated a maximum velocity of 0.193m/s at a 35cm vertical distance above the head, which is 1% and 10% higher than the mouth-breathing case and nose breathing case, respectively (Fig. 18). The non-breathing case also generates a higher maximum velocity and has a less vertical distance to the point with maximum velocity from the head compared to two other breathing cases. In general, the velocity gradient above the head, the maximum and minimum velocities are very similar for these three cases. At the 5cm vertical distance above the head, the velocity of the central point is smaller to the velocity in other horizontal directions. According to the previous studies, the central point is inside the CBL. At the 10cm vertical distance above the head, the velocity of the central point

is two times bigger than it at the lower measuring point, which means the measuring point is out of the convective boundary at this height. However, the changes in the thickness of convective boundary need to be studied in the future.

5. Conclusion

The main conclusions arising from the experimental investigation performed in a quiescent indoor environment are as follows:

- At a 23°C indoor air temperature, in non-breathing case, the velocity reached its highest value around 0.193m/s at an approximately 35cm vertical distance above the head. At a 5cm lateral distance in front of the manikin, the velocity reached the highest value at chest height level.
- Taking the breathing into account when performing experiments weakened the thermal gradient, which the nose breathing case had more impact on velocity around the sitting manikin than the mouth-breathing case.
- Above the manikin's head, the velocity in the non-breathing case had little difference with that in the breathing cases. But, in comparison with other cases, the velocity in the non-breathing case had the higher maximum velocity value and the shortest vertical distance to reach the maximum velocity.
- Experiments on the real human verified the accuracy of the manikin's experiments. The mean velocity caused by the real human was, indeed, similar to the velocity generated by manikin.
- Considering the distribution of pollutants around the manikin, nose breathing may provide a higher air quality in the breathing zone.

To further understand the behavior of the thermal plume around the human body, it is necessary to study its interaction with airflow generated by ventilation system because, in most cases, the indoor environment is impossible to stay in a quiescent condition. Since the present study excludes the pollutants concentration and distribution, the future work will be focused on the pollutants concentration and distribution for different breathing methods, and how to improve the air quality in the breathing zone.

Funding

We thank Energy and Indoor Environment Laboratory at the Department of Energy and Process Engineering at Norwegian University of Science and Technology and China Scholarship Council for providing financial support.

Acknowledgments

We thank Energy and Indoor Environment Laboratory at the Department of Energy and Process Engineering at Norwegian University of Science and Technology for providing technical support, and all the volunteers for real human experiments. The authors wish to also express their gratitude to Mehrdad Rabani, from OsloMet-Oslo Metropolitan University, for his contribution to experiments.

Conflicts of interest

There are no conflicts of interest to declare.

Reference

- [1] Etheridge D. and Sandberg M. (1996) *Building Ventilation: Theory and Measurement*, John Wiley and Sons Ltd, Chichester, England;
- [2] Parsons, K. (2003). *Human thermal environments: The effects of hot, moderate, and cold environments on human health, comfort, and performance*. CRC Press.
- [3] Vander, A. J., Sherman, J. H., and Luciano, D. S., 1994, *Human Physiology: The Mechanisms of Body Function*, McGraw-Hill, Inc., New York.
- [4] ISO, International Standard ISO/DIS/7730 (2005) *Moderate Thermal Environments- Determination of PMV and PPD Indices and Specification of the Conditions for Thermal Comfort: International Standard Organization for Standardization, Geneva, Switzerland;*
- [5] ANSI/ASHRAE Standard 55. *Thermal environmental conditions for human occupancy*. American Society of Heating, Refrigerating and Air-Conditioning Engineers, Inc; 2017.
- [6] Bjørn E, Nielsen PV. Dispersal of exhaled air and personal exposure in displacement ventilated rooms. *Indoor Air* 2002;12(3):147–64.
- [7] Johnson AE, Fletcher B, Saunders CJ. Air movement around a worker in a low-speed flow field. *The Annals of Occupational Hygiene* 1996;40(1):57–64.
- [8] Xing H, Hatton A, Awbi HB. A study of the air quality in the breathing zone in a room with displacement ventilation. *Building and Environment* 2001;36(7):809–20.
- [9] Murakami S, Kato S, Zeng J. Combined simulation of airflow, radiation and moisture transport for heat release from a human body. *Building and Environment* 2000;35(6):489–500.
- [10] Clark RP, Toy N. Natural convection around the human head. *J Physiol* 1975; 244(2):283-93.
- [11] Zukowska D, Popiolek Z, Melikov A. Determination of the integral characteristics of an asymmetrical thermal plume from air speed/velocity and temperature measurements. *Exp Therm Fluid Sci* 2010;34(8):1205-16.
- [12] Licina, D., Pantelic, J., Melikov, A., Sekhar, C., Tham, K. W. Experimental investigation of the human convective boundary layer in a quiescent indoor environment. *Building and Environment* 2014; 75: 79-91.
- [13] Spitzer, I.M., D.R. Marr, M.N. Glauser, Impact of manikin motion on particle transport in the breathing zone. *Journal of Aerosol Science*, 2010. 41(4): 373-383.
- [14] Zukowska, D., A. Melikov, Z. Popiolek, Impact of personal factors and furniture arrangement on the thermal plume above a sitting occupant. *Building and Environment*, 2012. 49: 104-116.
- [15] Voelker, C., Maempel, S. and Kornadt, O. Measuring the human body's microclimate using a thermal manikin. *Indoor Air*, 2014. 24: 567-579. doi:10.1111/ina.12112
- [16] Xu, C., P. V. Nielsen, L. Liu, R. L. Jensen, G. Gong. Human exhalation characterization with the aid of schlieren imaging technique. *Building and Environment*, 2017. 112: 190-199.
- [17] Craven, B.A. G.S. Settles, A Computational and Experimental Investigation of the Human Thermal Plume. *Journal of Fluids Engineering*, 2006. 128(6): 1251-1258.
- [18] Clark, R.P., and Edholm, O.G. (1985) *Man and his thermal environment*, E. Arnold, London
- [19] Clark, R.P. and de Galcina-Goff, M.L. (2009) Some aspects of the airborne transmission of infection, *Journal of the Royal Society Interface*; 6, S767-S782
- [20] Laverge, J., M. Spilak, and A. Novoselac, Experimental assessment of the inhalation zone of standing, sitting and sleeping persons. *Building and Environment*, 2014. 82: 258-266.
- [21] Allen, R. *The health benefits of nose breathing*. *Nursing in General Practice*, 2015.

- [22] Hyldgaard CE. Humans as a source of heat and air pollution. In: Proceedings of the 4th International Conference on air distribution in rooms e Roomvent 1994, Cracow, Poland, vol. 1; 1994. 413-33.
- [23] Melikov A. Breathing thermal manikins for indoor environment assessment: important characteristics and requirements. *Eur J Appl Physiol* 2004;92(6): 710-3.
- [24] Hyldgaard CE. Thermal plumes above a person. In: Proceedings of the 6th International Conference on air distribution in rooms e Roomvent 1998, Stockholm, Sweden, vol. 1; 1998. 407-13.
- [25] Rim D, Novoselac A. Transport of particulate and gaseous pollutants in the vicinity of a human body. *Build Environ* 2009;44(9):1840-9.
- [26] OSHA Lead in Construction Advisor (2015) by U.S. Department of Labor
- [27] Glossary of Environment, Safety, and Health Terms (2006) by U.S. Department of Energy
- [28] Lewis HE, Foster AR, Mullan BJ, Cox RN, Clark RP. Aerodynamics of the human microenvironment. *Lancet* 1969;322(7609):1273-7.
- [29] Licina D, Melikov A, Sekhar C, Tham KW. Air temperature investigation in microenvironment around a human body. *Building and Environment*. 2015;92:39-47